Camera Calibration and Stereo via a Single Image of a Spherical Mirror

Nissim Barzilay ⬤ , Ofek Narinsky ⬤, and Michael Werman ⬤

e-mail: *nissim.barzilay*@mail.huji.ac.il

ofek.narinsky@mail.huji.ac.il

michael.werman@mail.huji.ac.il

Abstract—This paper proposes a technique for camera calibration and depth estimation from a single view that incorporates a spherical mirror. By leveraging the sphere's contour and reflections, the approach enables precise calibration and scene measurement while capturing additional environmental details beyond the direct image frame. The study explores the geometry and calibration of catadioptric stereo systems, addressing both challenges and practical applications. The paper delves into the intricacies of the geometry and calibration procedures involved in catadioptric stereo utilizing a spherical mirror. Experimental results with synthetic and real-world data demonstrate the method's feasibility and accuracy.

Keywords-Camera matrix calibration; Single-view image; Spherical objects; Mirror sphere; Computer vision.

I. Introduction

Incorporating spherical mirrors in a catadioptric imaging system makes it possible to observe a wide area with a relatively small mirror. Research and analysis of catadioptric systems based on spherical mirrors can be found in various papers [1]–[3].

Inspired by the concepts introduced in [4], [5], which utilized two spheres in the camera's field of view for obtaining stereo information, our focus is on the more practical scenario of employing a single mirrored sphere. Our research aims to present a method capitalizing on the unique attributes of a single mirrored sphere for both camera matrix calibration and catadioptric stereo.

Our approach only requires the image to show part of the sphere's contour and one of the following; the reflection of the camera, two pairs of corresponding points on and off the spherical mirror, or a single correspondence in special cases.

This research extends to the practical implementation of a real-time system, showcasing the feasibility and efficacy of employing mirrors for stereo imaging as a compelling alternative to the established two-camera stereo methodologies. It is also applicable in scenarios where an accidental spherical mirror is present in the scene. In Section 2, reviews related work in catadioptric imaging system and existing calibration methods, highlighting the advantages and limitations of prior approaches. In Section 3, presents our proposed method for camera calibration and depth estimation using a single spherical mirror, including a detailed explanation of the mathematical formulation and implementation. In Section 4, provides experimental results, including synthetic and real-world data, to validate the accuracy and feasibility of our approach. Finally, In Section 5, discusses the implications of our findings, possible improvements, and potential real-world

Figure 1. Spherical mirror in scene

applications. It concludes the paper with a summary of our contributions and directions for future research.

II. Related Work

Catadioptric imaging systems, combining cameras with one or more mirrors, can be divided into categories based on the mirror type and calibration methods. A planar mirror, often used to create a new viewpoint, serves as a cost-effective option for building a stereo system with a single camera. In contrast, a spherical mirror provides a significantly wider field of view, making it popular in catadioptric systems that aim to capture a more complete environment.

Central catadioptric camera calibration: Central catadioptric cameras are imaging devices that use mirrors to enhance the field of view while preserving a single effective viewpoint[6]. Linear calibration methods are proposed that unify the handling of straight-line projections in the real world and sphere images formed by reflections of a spherical mirror, requiring three images of a spherical mirror for implementation. Ying et al. propose a calibration method for paracatadioptric camera based on sphere images, which only requires that the projected contour of a parabolic mirror is visible on the image plane in one view [7]. Their approach relies on the projection properties of spheres in central catadioptric cameras, utilizing a unit viewing sphere model where a sphere projects to two parallel circles they derive constraints for camera calibration. Our method is not sufficient for a central catadioptric camera calibration due to our assumption that the sphere projects an ellipse in the image.

Multiple views of spheres: Agrawal et al. [8], [9] and Zhang [10] developed comprehensive methods for camera calibration, positioning three or more spheres at multiple locations. They present an algorithm that uses the projection of the occluding contours of three spheres and solves for the intrinsic parameters and the locations of the spheres. Extrinsic calibration here involves first estimating each sphere's 3D position in the camera's coordinate system, using known intrinsic parameters and projected ellipses. The methods then determine relative rotation and translation between cameras by aligning these 3D sphere centers. Schnieders et al. [11] propose a method that given multiple views of a single sphere, estimate the camera parameters using the recovered sphere and light directions.

Mirror-Based Calibration with a single-view image: Calibration algorithms that do not require direct observation of 3D reference objects. Many approaches leverage Zhang's calibration algorithm to estimate intrinsic parameters, For instance, Francken [12] utilized this approach for webcam calibration restricted to a screen setup, and others, like Agrawal [13], adapted similar methods.

Perhaps the closest work to our topic is presented by Han et al. [14], who propose a novel self-calibration method for single-view 3D reconstruction using a mirror sphere. Han's approach requires estimating/guessing both the principal point and focal length from a single-view image by minimizing focal length discrepancies between images or through iterative sampling. In contrast, our method computes camera intrinsic parameters directly based on precise mathematical equations derived from the sphere's contour and reflection properties. This approach enables a robust calibration process that avoids iterative estimation, making it suitable for real-time applications.

III. METHOD

In this paper, we assume:

- A projective camera with no skew.
- The image contains a spherical mirror.
- The extrinsic parameters of the camera are

$$\begin{bmatrix} 1 & 0 & 0 & 0 \\ 0 & 1 & 0 & 0 \\ 0 & 0 & 1 & 0 \end{bmatrix} \tag{1}$$

- The unit is defined by the sphere's radius.

To calibrate the camera we need to find the sphere's contour and center in the image. The sphere projects to an ellipse in the image [15]. Let the conic be $v^T C v = 0$, where T denotes transposition, with v the homogeneous coordinates of a point on the conic, and C is the 3×3 symmetric matrix (as illustrated in Figure 1, where the ellipse mark in red represents the projected contour of the sphere.).

Locating ellipses in images is a long-studied challenge, with various methods proposed to tackle it, including both traditional and deep learning approaches, for example, [16]–[19].

Next, we find the sphere's center in the image ($O = \begin{bmatrix} o_x & o_y & 1 \end{bmatrix}^T$). O can be determined by either of the following three methods:

1) Locating the camera's reflection in the mirror (see Figure 9a, Figure 9b). The rays from the camera to the mirror, from the mirror to the camera and the normal at the mirror coincide, thus the ray from the camera to its reflection in the mirror intersects the center of the sphere. So, the image of the camera center is also the location of the *image* of the sphere's center.
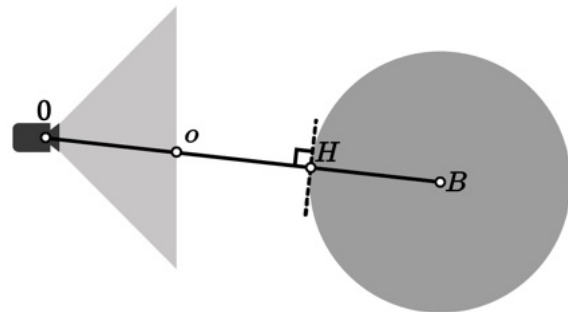

(a) The rays from the camera to the mirror $0 \to H$, from the mirror to the camera $H \to 0$, and the normal at the mirror coincide.

(b) The center of the sphere in the image is at the camera's reflection.

Figure 2. Illustration of method 1.

2) Using 2 or more pairs of correspondence points (see Figure 3a, Figure 3b). Let v be the image of a 3D point V and v' the image of V's reflection at V' then the rays from the camera to V', from V' to V and from V' to the sphere's center B (the normal) are coplanar and include the camera center thus project to the line in the image coincident to the sphere's center. The intersection of lines spanning corresponding points, on and off the mirror, is thus the image of the sphere's center.

3) If we assume that the camera has equal focal lengths, $f_x = f_y$. intersecting the line containing a single pair of corresponding points and the major axis of the ellipse, (see Figure 4) suffices. This follows from the *axial* constraint [15], which is the observation that the camera
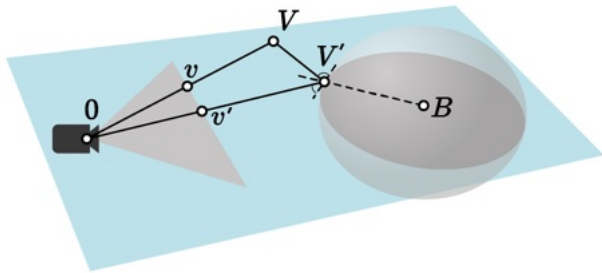
(a) A 2D cross-section of a pair of correspondence points.

(b) Finding the sphere's center in the image from two pairs of corresponding points.

Figure 3. Illustration of method 2.

Figure 4. Finding the sphere's center from a single pair of corresponding points and the major axis of the ellipse. The green line connects the corresponding points, while the red line represents the major axis of the ellipse.
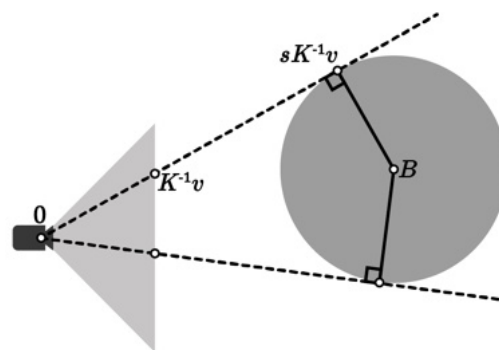
Figure 5. 2D example of sphere outline. $sK^{-1}V$ is perpendicular to $B - sK^{-1}V$. The distance between $sK^{-1}V$ and B is the radius, which is 1.

center, the sphere center, and the major ellipse axis are co-planar. Thus, the image of the sphere center is on the ellipse's major axis.

We want to compute the camera matrix $P_{3\times4}$ and the sphere's center $B = \begin{bmatrix} b_x & b_y & b_z \end{bmatrix}^T$. We will use the radius of the sphere as the unit. Assuming a no skew camera

$$P := \begin{bmatrix} f_x & 0 & t_x & 0 \\ 0 & f_y & t_y & 0 \\ 0 & 0 & 1 & 0 \end{bmatrix} = \begin{bmatrix} \mathbf{K} & \begin{matrix} 0 \\ 0 \\ 0 \end{matrix} \end{bmatrix} \quad (2)$$

K contains the first 3 columns from the matrix P. Where f_x, f_y are the focal lengths and (t_x, t_y) is the principle point.

Let $V = \begin{bmatrix} v_x & v_y & 1 \end{bmatrix}^T \in \mathbb{R}^3$ be a pixel on the projected contour of the sphere. Geometrically (see Figure 5) this means that there is $s \in \mathbb{R}^+$ such that:

- $\triangle 0, sK^{-1}V, B$ is a right triangle.
 In other words

$$\langle sK^{-1}V, B - sK^{-1}v \rangle = 0. \quad (3)$$

- The distance between $sK^{-1}V$ and B is the radius. The radius is our unit, so

$$|sK^{-1}V - B| = 1 \quad (4)$$

We simplify these equations to get:

$$\langle K^{-1}V, B \rangle^2 + (1 - |B|^2)|K^{-1}V|^2 = 0 \quad (5)$$

We use the fact that an inner product can be represented by a matrix multiplication and rewrite it as:

$$V^T K^{-T}(BB^T + (1 - |B|^2)I)K^{-1}V = 0 \quad (6)$$

Where I denotes the identity matrix ensuring that it preserves the dimensional of B. This is an equation of the conic section we already computed: C. Therefore, they are equivalent up to a scalar factor:

$$C = rK^{-T}(BB^T + (1 - |B|^2)I)K^{-1} \quad (r \in \mathbb{R}) \quad (7)$$

We currently have 8 unknowns:

$$r, b_x, b_y, b_z, f_x, f_y, t_x, t_y$$

but equating the conic sections only gives 6 equations (Both matrices are symmetric). We first get rid of t_x, t_y by shifting the image so $(0,0)$ represents the center of the sphere. We define:

$$S := \begin{bmatrix} 1 & 0 & o_x \\ 0 & 1 & o_y \\ 0 & 0 & 1 \end{bmatrix} \quad (8)$$

Since we know C, o we can compute the matrix

$$M := S^T C S \tag{9}$$

$$Q := b_z K^{-1} S = \begin{bmatrix} b_z f_x^{-1} & 0 & b_x \\ 0 & b_z f_y^{-1} & b_y \\ 0 & 0 & b_z \end{bmatrix} \tag{10}$$

$$p = \frac{r}{b_z^2} \tag{11}$$

We get:

$$M = pQ^T(BB^T + (1 - |B|^2)I)Q \tag{12}$$

Denote $m_{ij} := M[i, j]$. can be expanded to a system of equations:

$$\begin{cases} m_{11} = pf_x^{-2}b_z^2(b_x^2 + 1 - |B|^2) \\ m_{22} = pf_y^{-2}b_z^2(b_y^2 + 1 - |B|^2) \\ m_{33} = p|B|^2 \\ m_{12} = pf_x^{-1}f_y^{-1}b_xb_yb_z^2 \\ m_{13} = pf_x^{-1}b_xb_z \\ m_{23} = pf_y^{-1}b_yb_z \end{cases} \tag{13}$$

To solve these equations, first calculate p and $|B|^2$:

$$p = \frac{m_{13}m_{23}}{m_{12}} \tag{14}$$

,

$$|B|^2 = \frac{m_{33}}{p} \tag{15}$$

Now we can calculate b_x^2, b_y^2, b_z^2:

$$b_x^2 = \frac{1 - |B|^2}{\frac{m_{11}}{m_{13}^2}p - 1}, \quad b_y^2 = \frac{1 - |B|^2}{\frac{m_{22}}{m_{23}^2}p - 1}, \quad b_z^2 = |B|^2 - b_x^2 - b_y^2 \tag{16}$$

The choice of either the positive or negative square root of b_x^2, b_y^2 doesn't matter and it will be compensated by positive or negative f_x, f_y. However, b_z should be positive as the sphere is in front of the camera. Now we can determine the values of f_x, f_y:

$$f_x = \frac{pb_xb_z}{m_{13}}, \quad f_y = \frac{pb_yb_z}{m_{23}} \tag{17}$$

Notice KB is the position of the sphere's center in the image, so $KB = b_zo$. Therefore, we can determine the values based on our previous calculations:

$$t_x = o_x - f_x\frac{b_x}{b_z}, \quad t_y = o_y - f_y\frac{b_y}{b_z} \tag{18}$$

Note that knowing both the sphere's and camera parameters suffice to reconstruct the $3D$ positions of all pairs of corresponding points by intersecting the corresponding rays.

Figure 6. Synthetic Data 1

IV. RESULTS

We have tested our algorithm on a synthetic image of resolution 2048x2048 generated using Blender (see Figure 6), using only the conic section, the contour of the spherical mirror, and the reflection of the camera to calibrate the image.

First phase: We selected points on the sphere contour and calculated the conic. Second phase: We estimate the center of the sphere in the image by locating the camera's reflection. Now we apply our algorithm to calibrate the image. Figure 7 resolution 1920x1080.

TABLE I. COMPARISON OF REAL VALUES AND OUR ALGORITHM'S RESULT ON 6.

	Parameters	
	$b_x = 3$	$b_y = -4,$
Ground Truth	$b_z = 7$	$f_x = 1024$
	$f_y = 1024$	$t_x = 1024$
	$t_y = 1024$	
	$b_x = 3.00$	$b_y = -3.94$
Result	$b_z = 7.03$	$f_x = 1027.99$
	$f_y = 1032.84$	$t_x = 1024.34$
	$t_y = 1016.94$	
Error Range	Less than 1.5%	

TABLE II. COMPARISON OF REAL VALUES AND OUR ALGORITHM'S RESULT ON 7.

	Parameters	
	$b_x = -1.5$	$b_y = 3,$
Ground Truth	$b_z = 1$	$f_x = 1144$
	$f_y = 1144$	$t_x = 960$
	$t_y = 540$	
	$b_x = -1.47$	$b_y = 3.07$
Result	$b_z = 1$	$f_x = 1179$
	$f_y = 1167$	$t_x = 949$
	$t_y = 535$	
Error Range	Less than 3.1%	

Figure 7. Synthetic Data 2

In the real image 1600x1196 (see Figure 1), the estimated sphere origin is:

$$b_x = -0.76, \quad b_y = 0.13, \ b_z = 5.07$$

$$f_x = -1744, \quad f_y = 1732, \quad t_x = 722, \quad t_y = 583$$

To verify our algorithm, we also computed the length of objects using two pairs of correspondence points (Figure 3a) and a sphere with a radius of 5 cm, in Figure 8. We computed the height of the vase using two pairs of corresponding points. We computed the ray for each point. Let v,v', and u, u' be pairs of correspondence points; we then calculate the rays in 3D space. This conversion involves scaling and translating the pixel coordinates. Next, we compute the 3D point representation where the ray intersects the correspondence point v', denoted as h. According to the equation we presented earlier, (4), we define offset $= h - B = sK^{-1}V - B$ with the condition $|sK^{-1}V - B| = 1$. The reflected vector is

$$\text{reflect} = h - 2 * \langle \text{offset}, h \rangle * \text{offset}.$$

Given the reflected ray and the direct ray, we compute the 3D position of the point. The first and second phases are the same as described in the previous example.

$$b_x = 1.30, \ b_y = 0.48, \ b_z = 5.62$$

$$f_x = 2714, \ f_y = 2703 \quad, \quad t_x = 3052, \ t_y = 1664$$

The height of the marker is 13cm, computing the 3D points of v, u marked in red and their distance we obtained is a height of 14 cm. The real height of the tape dispenser is 5cm, computing the 3D points of v, u marked in blue and the distance we calculated a height of 5.05 cm.

TABLE III. COMPARISON OF ZHANG EVALUATION FOR OVER MORE THEN 20 IMAGES AND OUR ALGORITHM'S ON A SINGLE IMAGE RESULT

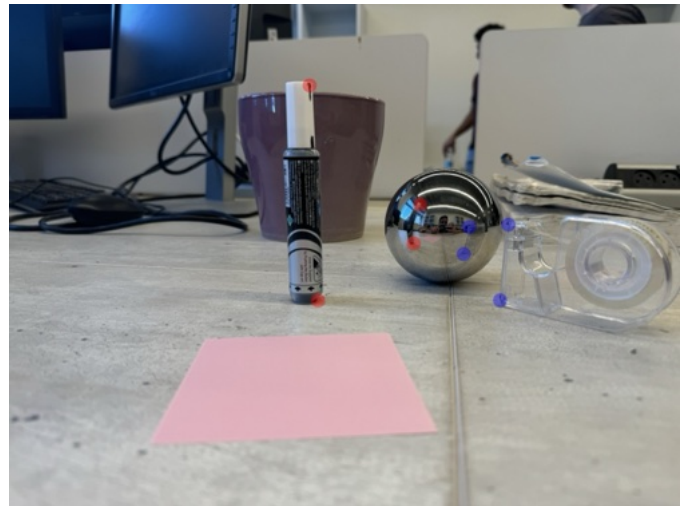|		Parameters		
9.	Zhang Calibration	$f_x = 8146$		
		$f_y = 8286$	$t_x = 3143$	$t_y = 2397$
	Result	$f_x = 8258$		
		$f_y = 8073$	$t_x = 3904$	$t_y = 3875$

Figure 8. Height test

(a) Single image of a spherical mirror - our algorithm

(b) Images - Zhang algorithm

Figure 9. Comparison of Camera Calibration Methods for the Canon EOS R10

V. CONCLUSION AND FUTURE WORK

We presented a novel approach for calibrating the camera matrix using a single-view image. Our findings help reduce the requirements for achieving this calibration. Using our method, further image analysis is possible, such as determining the 3D location of a point from a pair of corresponding points or estimating an omnidirectional image centered at the sphere's origin. Additionally, since a spherical mirror distorts the scene by projecting it onto a curved surface, we aim to leverage our findings to correct this distortion and reconstruct the scene as if it were reflected in a planar mirror in future work.

REFERENCES

[1] S. Barone, M. Carulli, P. Neri, A. Paoli, and A. V. Razionale, "An omnidirectional vision sensor based on a spherical mirror catadioptric system," *Sensors*, vol. 18, no. 2, 2018. DOI: 10.3390/s18020408.

[2] Y. Hiruta, C. Xie, H. Shishido, and I. Kitahara, "Catadioptric stereo-vision system using a spherical mirror," *Procedia Structural Integrity*, vol. 8, pp. 83–91, 2018, AIAS2017 - 46th Conference on Stress Analysis and Mechanical Engineering Design, 6-9 September 2017, Pisa, Italy, ISSN: 2452-3216. DOI: https://doi.org/10.1016/j.prostr.2017.12.010.

[3] Y. Hang, L. Zhao, and W. Hu, "A survey of catadioptric omnidirectional camera calibration.," *International Journal of Information Technology and Computer Science,*, 2013.

[4] S. Nene and S. Nayar, "Stereo with mirrors," in *Sixth International Conference on Computer Vision (IEEE Cat. No.98CH36271)*, 1998, pp. 1087–1094. DOI: 10.1109/ICCV.1998.710852.

[5] Y. Hiruta, H. Shishido, and I. Kitahara, "One shot 3d reconstruction by observing multiple spherical mirrors," in *2021 IEEE 10th Global Conference on Consumer Electronics (GCCE)*, 2021, pp. 580–584. DOI: 10.1109/GCCE53005.2021.9621989.

[6] X. Ying and H. Zha, "Identical projective geometric properties of central catadioptric line images and sphere images with applications to calibration," *International Journal of Computer Vision*, vol. 78, no. 1, pp. 89–105, Oct. 2007. DOI: 10.1007/s11263-007-0082-8.

[7] Y. Li and Y. Zhao, "Calibration of a paracatadioptric camera by projection imaging of a single sphere," *Appl. Opt.*, vol. 56, no. 8, pp. 2230–2240, Mar. 2017. DOI: 10.1364/AO.56.002230.

[8] Agrawal and Davis, "Camera calibration using spheres: A semi-definite programming approach," in *Proceedings Ninth IEEE International Conference on Computer Vision*, 2003, 782–789 vol.2. DOI: 10.1109/ICCV.2003.1238428.

[9] M. Agrawal and L. Davis, "Complete camera calibration using spheres : A dual-space approach," Jan. 2003.

[10] H. Zhang, K.-y. K. Wong, and G. Zhang, "Camera calibration from images of spheres," *IEEE Transactions on Pattern Analysis and Machine Intelligence*, vol. 29, no. 3, pp. 499–502, 2007. DOI: 10.1109/TPAMI.2007.45.

[11] D. Schnieders and K.-Y. K. Wong, "Camera and light calibration from reflections on a sphere," *Computer Vision and Image Understanding*, vol. 117, no. 10, pp. 1536–1547, 2013, ISSN: 1077-3142. DOI: https://doi.org/10.1016/j.cviu.2013.06.004.

[12] Y. Francken, C. Hermans, and P. Bekaert, "Screen-camera calibration using a spherical mirror," in *Fourth Canadian Conference on Computer and Robot Vision (CRV '07)*, 2007, pp. 11–20. DOI: 10.1109/CRV.2007.59.

[13] A. Agrawal, "Extrinsic camera calibration without a direct view using spherical mirror," in *2013 IEEE International Conference on Computer Vision*, 2013, pp. 2368–2375. DOI: 10.1109/ICCV.2013.294.

[14] K. Han, K.-Y. K. Wong, and X. Tan, "Single view 3d reconstruction under an uncalibrated camera and an unknown mirror sphere," in *2016 Fourth International Conference on 3D Vision (3DV)*, 2016, pp. 408–416. DOI: 10.1109/3DV.2016.50.

[15] T. Tóth and L. Hajder, "A minimal solution for image-based sphere estimation.," *Int J Comput Vis*, 2023.

[16] M. Cicconet, K. Gunsalus, D. Geiger, and M. Werman, "Ellipses from triangles," in *2014 IEEE International Conference on Image Processing (ICIP)*, IEEE, 2014, pp. 3626–3630.

[17] A. Fitzgibbon, M. Pilu, and R. B. Fisher, "Direct least square fitting of ellipses," *IEEE Transactions on pattern analysis and machine intelligence*, vol. 21, no. 5, pp. 476–480, 1999.

[18] C. Lu, S. Xia, M. Shao, and Y. Fu, "Arc-support line segments revisited: An efficient high-quality ellipse detection," *IEEE Transactions on Image Processing*, vol. 29, pp. 768–781, 2019.

[19] W. Dong, P. Roy, C. Peng, and V. Isler, "Ellipse r-cnn: Learning to infer elliptical object from clustering and occlusion," *IEEE Transactions on Image Processing*, vol. 30, pp. 2193–2206, 2021.